

# Global Localization of Mobile Robots by Reverse Projection of Sensor Readings

Hemanth Korrapati, K Madhava Krishna and Aditya Teja

**Abstract**— Global localization algorithms involve a search over all possible poses of the robot that can be typically over a large space in huge maps. Essentially it involves computing a posterior by seeing how probable are the obtained sensor readings at each of the discretized states in a map. Instead in this paper by reverse projecting the sensor readings from the obstacle boundaries onto the surroundings, a solution is obtained by searching over the space of obstacle boundaries than by a search in the discretized pose space. That this search over obstacle boundaries is considerably less if the ratio of free space to boundary space in a map is high is straightforward. However we also show theoretically that even when the boundary space exceeds the free space the computations due to the current method does not exceed those due to the popular Markov and Correlation based approaches to global localization. The comparative advantages are well documented in simulation section of the paper. The approach is able to consistently localize a laser equipped robot in our lab.

## I. INTRODUCTION

Global localization [1,2] is the problem of estimating the state (pose) of the robot in a known map without an initial estimate of its state. The challenge is that in the absence of an initial guess the problem cannot be modeled with unimodal probability distribution leading to a search over all possible poses or states of the robot. The search is inevitably exponential in state dimensions. This contrasts with local localization where a guess of the robot's pose is made [3,4]. Since this guess or prediction is corrupted due to system as well as measurement noise, local localization methods correct the prediction to a more reliable estimate through techniques involving Extended Kalman Filters and scan matching [4] among others. There is also a vast family of algorithms that simultaneously localize and build maps called SLAM that is beyond the purview of this paper.

In this paper we present a novel method of global localization based on reverse projection of sensor readings from obstacle boundaries. The essential advantage of this method is the computational savings it offers by zeroing onto the state of the robot quickly, thereby circumventing the need to perform a search over the set of all possible states as in [1,2]. This it does by associating intensities to the free cells onto which the reverse projected readings fall. The intensity peaks at locations from obstacles that are at the obtained sensor distance after incorporating visibility constraints. Intensities corresponding to various sensor readings are superposed and the areas with highest intensity are the best

location/pose estimates of the robot. By performing computations from only those cells that constitute the obstacle perimeter rather than for all the cells in the map it offers substantial savings in cost and provides a faster alternative over popular global localization methods.

We illustrate this motivation as follows.

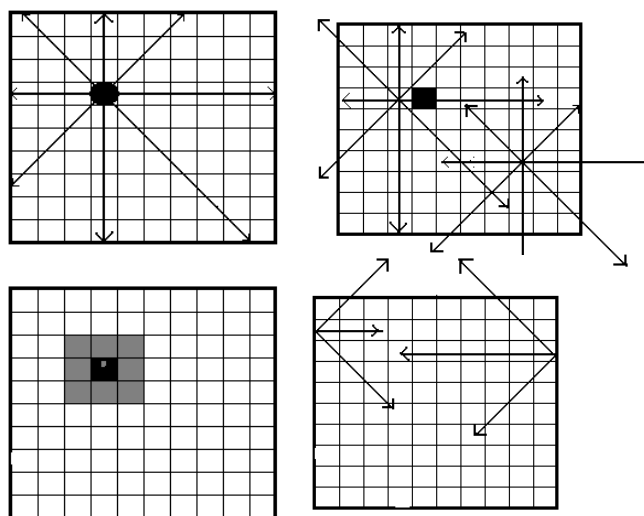


**Fig 1a (top left):** The map of a square environment, the shaded cell representing the robot, the boundary of the square the obstacles. Sensor readings are shown by arrows. The robot is unaware of its pose though. **Fig 1b (top right):** In the traditional method sensor measurements are projected from all possible states (cells) of the robot. The best state is that state where the projected measurements match what would have been the actual measurements obtained, within an error margin, had the robot been in that state. This computation is done for all free cells in the map. **Fig 1c (bottom left):** After the sensor scan the possible poses of the robot are shown by the shaded cells. **Fig 1d (bottom right):** In the current method sensor measurements are projected only from those cells that form the obstacle boundaries.

Figure 1a shows a square obstacle, the robot is in the shaded cell obtains sensor readings shown by lines. Global localization methods compute the posterior by computing how probable it was to have got these sensor readings at each of the discretized states in the prior. This is shown in figure 1b where the obtained sensor readings get projected at each of the prior states and compared with readings that would be obtained from there. The eventual posterior turns out to be the one shown in figure 1c.

In this paper we reduce the order of computation from number of cells in the freespace (those that are not occupied by obstacle) to those cells that constitute the boundary of the obstacle. This we do by projecting sensor measurements from the obstacle boundary onto the surrounding space while

This work was supported in part by a CARS grant from Center for AI and Robotics, Bangalore. The authors are with IIT-Hyderabad, India

the traditional global localization methods project the measurements from all points in the free space into the surrounding. This inverse operation, shown in figure 1d, would always be faster when compared with the traditional global localization methods. This has been analyzed both in theory and simulations where we have compared the current method with the popular Markov [1], particle filters [2] and correlation based approaches [5] for global localization. We also present arguments for the completeness of this method.

The paper is best viewed as a fast alternative to the first step computation of robot pose in global localization procedures. This method can quickly say those cells in the map where belief computations of [1] need to be done or those places where particles need to be initialized [2] instead of doing it across the entire terrain.

## II. LITERATURE REVIEW

The past decade has seen the problem been attacked in various ways, through grid based methods or Markov localization (ML) [1], particle filters [2], correlation methods [5] and topological methods [6]. Probabilistic global localization became popular through the seminal work of Fox [1] and Thrun [2], where the state of the robot is described as a distribution of cells or particles with probabilities. Earlier approaches have tackled the problem of localizing a robot in a polygonal map [7] that was later extended in an active localization context [8]. Soon after the paper of [1] a fast localization method based on correlation was proposed in [5]. This approach relied on correlating a sensor patch with the sensor readings that would have been obtained at each of the prior discretized state. It avoided the Gaussian computations of [1] while computing the posterior as well as avoided storing the shortest distance to the obstacle at each probable state of the robot. It did not consider visibility constraints and was hence not accurate as [1] but was faster. Later approaches tried to tackle the problem of large state space by adapting the number of particles (Adaptive Monte Carlo Localization-AMCL) as in [9] or by the Reverse Monte Carlo Localization (RMCL) as in [10]. The RMCL uses ML in its first stage to find the approximate region where the robot should be and further refines the estimate through a MCL in the region delineated by ML. In [11] a real-time particle filter method was divulged that allowed for making use of all sensor information even when the sensor refresh rates were faster than filter update rates.

However all the above approaches *do* involve a search in the set of all possible robot poses for the first iteration of their algorithms. The current method of searching in the space of obstacle boundaries by reverse projecting sensor readings from the obstacle boundaries is novel and does not seem to appear in literature. It is also backed by theoretical analysis apart from experimental comparisons as to why the method will be inherently faster.

### A Methodology

Given a workspace, populated with obstacles, the cells that constitute the boundary of obstacles are enumerated into the set  $C$ . Let any such cell be denoted as  $c_i$ ,  $i = \{1, 2, \dots, n\}$ ,  $c_i \in C$ . Let the sensor scan be represented as  $S$  and its  $m$  individual measurements as  $O_i$ ,  $i = 1$  to  $n$ , for each  $O_i$  there is associated with it an angle,  $\theta_i$ , the angle at which the measurement  $O_i$  was obtained with respect to a global reference frame  $G$ . Then for every  $c_i \in C$ , one way of computing the intensity from  $c_i$  due to  $O_i$  is as

$$I_{C_i}(r, \phi) = Ke^{-\left(\frac{|r-o_i|^2}{2\sigma_r^2} + \frac{|\phi-(\theta_i-\pi)|^2}{2\sigma_\theta^2}\right)} \quad (1)$$

Where  $r$  is the distance of the cell for which intensity is computed from  $c_i$  and  $\phi$  is the angle made by that cell with  $c_i$ . However in practice we find a Gaussian is not really required, any method of giving a high intensity at the cell at which  $O_i$  falls when projected along  $\theta_i - \pi$  and tapering off the intensities at cells in front and back suffices. Here we have tacitly neglected variance in  $\theta_i$  due to following reasons from the computation.

- I. For narrow angle measurement devices such as SICK LRF  $\sigma_\theta$  becomes almost redundant [1,2].
- II. Even for wide angle sensors such as sonar the method of extracting RCD from a sensor scan gets rid off the variance in  $\theta$  almost completely [13].
- III. Lastly and most importantly popular global localization methods have neglected  $\sigma_\theta$  when computing the posterior since the quality of the localization has not been affected and also to reduce computation. Since comparative analysis is one of the concerns of this paper the variance in the angle has been avoided in computations to maintain consistency across methods.

Thus for every cell  $c_i \in C$  and a given  $O_i, \theta_i$ , the region of influence of the measurement lies along  $\theta_i - \pi$ . We quantify this influence region as  $k = \sigma_r/g$ , where  $g$  is the cell resolution and  $k$  the number of cells that need to be updated due to variance in the distance measured. This is shown in figure 2a. The cell at which the sensor reading projected from the left obstacle boundary falls receives the highest intensity. Cells on either side get lesser intensities, here  $k=5$ . Discrete values of intensity obtained are added to the previous intensity values. The cells with highest intensity are most possible poses of the robot. This in short summarizes the localization method based on reverse projection. The philosophy is depicted in fig 2b. The location of highest

intensity is the meeting place of maximum arrows and denotes the place of highest likelihood of localization.

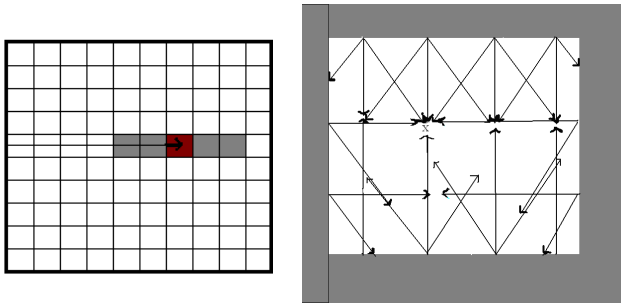


**Fig2a (left):** A sensor reading is reverse projected from the left obstacle boundary. The location where the reading falls has the highest intensity and shown darkest Cells on either side get progressively lesser intensity shown by lighter cells. Here  $k=5$ . **Fig 2b (right):** The cells experience highest intensity where most of the arrows converge. This is the most likely pose of the robot.

### B Computational Comparisons

We make extensive computational comparisons down to the detail between the Markov and current method.

*Computations for the Markov method with  $n$  free cells and  $m$  sensors on the robot for each free cell:*

1.  $m$  subtractions and additions of form  $(r_1 - o_1)^2 + (r_2 - o_2)^2 + \dots + (r_m - o_m)^2$
2.  $m$  squaring operations for terms like  $(r_i - o_i)^2$ .
3.  $m$  operations for finding shortest distance along direction of  $o_i$ .
4. One operation for a Gaussian computation or equivalently one gaussian computation

Hence the total number of operations for standard Markov method turns out to be:

1.  $mn$  operations for finding shortest distance at  $o_i$ , along  $\theta_i$
2.  $mn$  additions and subtractions
3.  $mn$  squaring operations.
4.  $n$  gaussian operations.

Hence the total number of operations equals  $n(2m+1)$  and number of computations (additions and subtractions) equals  $2mn$ .

*Worst Case Computations for Reverse Projection method: ( $p$  boundary cells,  $m$  sensors)*

Let  $\sigma_r$  = variance of a range measurement,  $g$  = cell resolution, and  $k = \lceil 2\sigma_r/g \rceil$ , where  $\lceil \cdot \rceil$  denotes the ceiling operator. For each boundary cell we have

1.  $m$  operations for finding nearest obstacle along  $\theta_i - \pi$  for a range measurement  $o_i$ .
2.  $m$  operations for finding cell indices and corresponding intensity values of cells for a reading  $o_i$  along  $\theta_i - \pi$ .

Thus the total number of operations is  $2mp$  and number of addition operations is  $kmp$ .

Hence the condition for operations to be less than the Markov method is  $2mp < 2mn$ . This is easily achieved if  $p < n$ . However in maps where  $p > n$  or the number of boundary cells are more than free cells the number of operations in the current method will yet be less than or equal to the Markov method. Due to space constraints we are unable to give the complete proof herewith. However we give a brief outline or sketch of the proof in the next section. It is to be noted that the computations derived for the current method are for worst-case scenarios while those for Markov method is always true. This is due to the following reasons:

1. The value of  $k$  that governs the number of cells to be updated represents its maximum value; in other words due to presence of obstacles along  $\theta_i - \pi$  the number of cells to be updated will only be less than  $k$ .
2. If the distance to the closest obstacle along  $\theta_i - \pi$  from  $c_i$  is less than  $o_i$  then  $k=0$ . Equivalently not all  $m$  sensor measurements give rise to intensity at a particular free cell due to presence of objects in between and hence updates need not happen for all  $m$  from  $c_i$  but only a fraction of it.

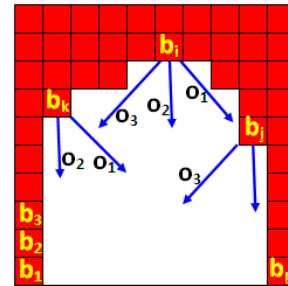


**Fig 3:** Figure showing reverse projections of sensor readings from boundary cells.

### III THEORETICAL RESULTS

We idealize a cell to a point or a pixel. The idealization is used to prove claims that otherwise are difficult to prove considering the very statistical nature of the problem at hand. Despite the idealization the theoretical results derived, serve as a sufficient backing to the simulation results portrayed in the next section.

Figure 3 depicts the reverse projection of sensor readings from some of the boundary cells. Let  $o_i$  represent the  $i^{th}$  sensor projection from any cell  $b_j$ ,  $i \in \{1, 2, \dots, m\}$ ,  $j \in \{1, 2, \dots, p\}$ . We denote three such measurements  $o_1, o_2, o_3$  for cells  $b_1, b_2$  and  $b_3$ . The following observations can be made, namely:

*Observation A (Obs A):* Any sensor measurement  $o_i$  would not intersect with any other sensor measurement  $o_k$  emanating from the same cell  $b_j$  inside the map  $M$ , except at the same cell  $b_j$  from where they diverge.

*Obs B:* Also that any sensor measurement  $o_i$  will not intersect with the same sensor measurement  $o_i$  from a different cell  $b_k$  since  $o_i$  emitted from  $b_j$  and  $b_k$  are parallel emitted at the same angle  $\theta_i - \pi$

The above two observations lead to the following lemmas and theorems that we state without proof due to brevity of space.

*Lemma 1:* In the reverse projection method there cannot be more than  $m$  intersections at any of the  $n$  free cells abstracted to point or pixel cells.

*Theorem 1:* For maps with point or pixel cells the number of computations due to the current method is always lesser than that due to Markov or Correlation approaches

The proof follows from *Lemma 1* that at each of the  $n$  cells there cannot be more than  $m$  intersections. Hence there can be at most  $m$  computations at each of the  $n$  cells. Therefore there will *not* be more than  $mn$  computations inside a map  $M$ , which is the number of computations due to Markov or correlation approaches.

#### IV SIMULATION RESULTS

Figure 4a shows the map of the environment and the pose of the robot in MobileSim, a mobile robotic simulator from Mobile Robots Inc. The robot has 8 sonar sensors, 6 in front and two at the rear, simulating Mobile Robot Inc's Amigobot. Only 8 range measurements were used for localization. Figure 4b shows the pose as returned by the current method. Dark regions show where the intensity of the occupancy is higher and lighter regions show where it is low. The cell that corresponds to the highest intensity is indicated by the green arrow. The error in the estimate was between 3-5% on an average for similar measurement errors. Figures 5a and 5b show a more complex map with the robot and the corresponding intensity. The region of highest intensity encircled in blue in 5b coincides with the location of the robot. Figures 5c and 5d show the 3D intensity plot in top view and rear side view. The region of peak intensity is shown by green arrow in both figures. These simulations verify the repeatability of the algorithm to yield accurate results.

Table 1 compares the current method vis-à-vis the Markov and correlation approaches for various values  $k$  and  $p/n$  ratios. Cells in column 1 specify the approach and column 2 specify the ratio of boundary to free cells ( $p/n$  ratios). As we go down the column this ratio keeps increasing. Columns 3 – 6 specify the time taken by the methods for a given percentage of measurement noise. The number of cells corresponding to this noise is denoted by the parameter  $k$  as before.

Increasing  $k$  values suggest more free cells need to be updated along the ray projected from the boundary cell indicative of increasing measurement noise. It can be seen for low values of  $p/n$  ratios the current approach is at-least 25 times faster than Markov approach and 8 times faster than correlation method. Increasing  $k$  does not increase the time taken by the current method in any noticeable way, thus the current algorithm continues to be significantly faster even as  $k$  increases when  $p/n$  is low.

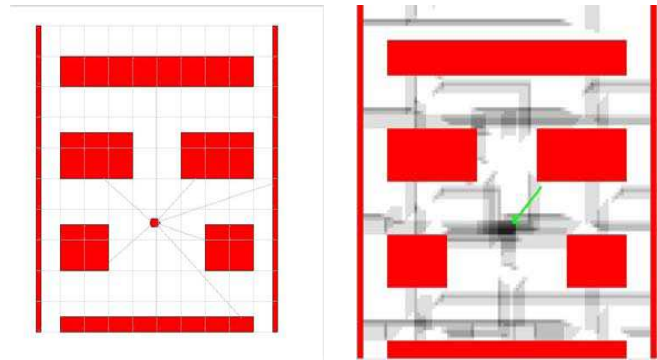


**Fig 4a(left):** A different map with both obstacles and robot in red. The robot is in the center and is the smallest of all the red objects. **Fig 4b (right):** The intensity plot. The maximum intensity region is shown marked by the arrow corresponds to the most likely pose of the robot.

As  $p/n$  increases the time taken by other methods decrease while that by the current method increases as expected. However even when  $p/n$  values are high (1 or more) the current method is 2.5 times faster than Markov method and becomes comparable to Correlation only at  $p/n=120\%$ . At  $p/n=100\%$  it is still 1.2 to 1.4 times faster than the correlation approach.

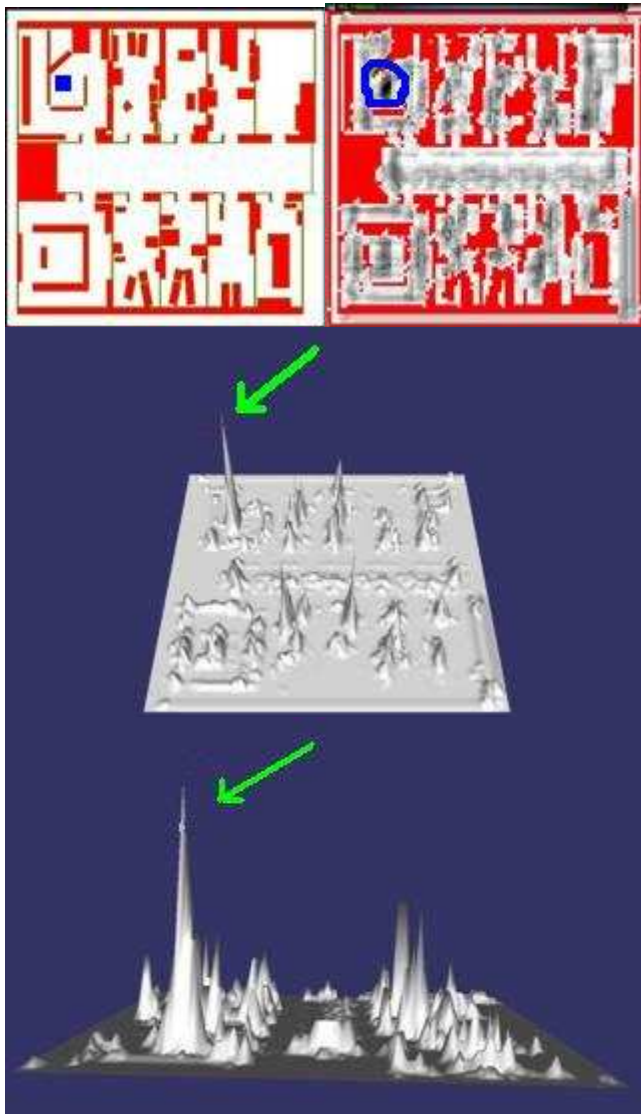
Increasing  $k$  has practically no effect at high  $p/n$  since there is hardly any free space and often there is only one cell along a direction to update, hence  $k$  is constrained at 1 even if measurement noise is higher. The average time in the tables is computed over several localization runs across various maps of similar scale and for various robot positions for the same map.

Table 2 shows the comparative trend when orientation is also estimated along with coordinates. The orientation results are tabulated for  $k$  values corresponding to 10% measurement noise. The trends are almost similar as in the previous cases. The current method is significantly faster for low values of  $p/n$ , it becomes comparable to Correlation at high values but continues to be faster than Markov by 1.2 times. MC runs are not shown for conserving space but their values were almost same as Markov.

Similar results were obtained for maps of smaller scales that are not shown here for brevity of space. All the above comparisons were performed on an Intel dual-core processor on Fedora Core 7. The small scale maps were of average size 200X200 while large scale maps were of an average size 1200X1200.

#### V IMPLEMENTATION RESULTS

The results of the reverse projection based global localization method were tested on our robot SPAWN that was built in house. The SPAWN is equipped with the SICK Laser Measurement System (LMS) and a pan-tilt stereo head. For the experiments here the LMS is used. The resolution of the laser was set at 1 degree resulting in 180 measurements in the frontal plane of the laser. The path of the robot is shown in figure 6a as it moves along a corridor



**Fig.5a(top left):** Showing the map of the environment and the robot's actual position in green. **Fig.5b(top right):** The intensity field obtained after running the algorithm on the map of fig.5a. The highest intensity point is circled in blue. **Fig.5c(middle row):** The top view of the 3D plot of the intensity field. **Fig.5d(last row):** The rear side view of the intensity field plotted in 3D. The point of highest intensity is pointed by the green arrow in 5c and 5d.

TABLE 1  
RUN-TIMES TAKEN ON LARGE SCALE MAPS

Method	p/n (%)	Time to localize in seconds for K values corresponding to a measurement noise percentage				
		K=5%	K=10%	K=15%	K=20%	K=25%
Markov		15.770	15.770	15.770	15.770	15.770
Correlation	10	1.754	3.543	4.678	5.452	6.116
Current Method		0.542	0.563	0.580	0.591	0.599

Markov		12.369	12.369	12.369	12.369	12.369
Correlation	25	1.543	2.848	3.763	4.128	4.442
Current		0.585	0.594	0.608	0.634	0.653
Markov		9.367	9.367	9.367	9.367	9.367
Correlation	50	1.324	1.876	2.321	2.456	2.522
Current		0.712	0.766	0.796	0.823	0.876
Markov		3.692	3.692	3.692	3.692	3.692
Correlation	100	1.110	1.385	1.448	1.523	1.602
Current		1.011	1.112	1.184	1.241	1.332
Markov		2.554	2.554	2.554	2.554	2.554
Correlation	120	0.960	0.963	0.963	0.964	0.964
Current		0.947	0.953	0.961	0.965	0.968

TABLE 2  
RUN-TIMES TAKEN ON A 100x100 MAP WITH UNKNOWN ORIENTATION FOR A K VALUE CORRESPONDING TO 10% NOISE

Method	p/n (%)	Run-Times (in seconds)
Markov		14.770
Correlation	10	13.540
Current Method		3.578
Markov		12.369
Correlation	25	11.263
Current Method		4.277
Markov		9.367
Correlation	50	8.873
Current Method		4.856
Markov		6.692
Correlation	100	6.213
Current Method		5.139
Markov		5.128
Correlation	120	4.731
Current Method		4.539

and in narrow passages on the right of the corridor. It scans the environment at locations 1, 2 and 3 to globally localize. The images corresponding to these scans are shown in figures 6b-6d. Figures 6e-6g shows the intensity at cells for the scans at locations 1, 2 and 3 in figure 6a. It can be seen that the intensity maximum regions correspond very closely to the actual position of the robot confirming the efficacy of this method.

## VI CONCLUSIONS

A novel method of globally localizing mobile robots based on reverse projection of sensor readings is presented. Comparisons reveal that the current method is many times faster than Markov and correlation approaches based global localization. The pivotal idea is that by projecting sensor measurements from the obstacle boundary onto the surrounding space rather than from all points in the free space onto the surroundings considerable computational reductions can be achieved. Simulation and real time implementations on a LMS equipped mobile robot confirm the efficacy of the current method both in terms of accurate and fast localization. This method of reverse projection of sensor scan from perimeter of the obstacles has not appeared in the literature based on our survey. The simulation results vindicate the theoretical results obtained earlier that the current method would always have lesser or equal number of computations when compared with previous methods.

The current method can be perceived in two ways. Firstly it can be viewed as an aid to quick Markov or particle filter localization. Markov localization involves belief computation of robots position at all cells in a discretized representation of the map of the environment. Particle filters or Monte Carlo methods initialize particles across the whole map. This method can quickly say those cells in the map where belief computations need to be done or those places where particles need to be initialized instead of doing it across the entire terrain. Secondly, it is a faster alternative to traditional global localization methods based on Markov, Correlation and particle filter approaches. The method is best used as an alternative to the sensor update phase or the posterior computation phase when the prior has a uniform distribution across the entire pose space.

This method would find utility in all applications that entail global localization in large maps, all the more so if there is more free space than boundary space.

## REFERENCES

- [1] D. Fox, W. Burgard, and S. Thrun, "Active markov localization for mobile robots", *Robotics and Autonomous Systems.*, 25, 195-207, 1998
- [2] S. Thrun, D. Fox, W. Burgard, and F. Dellaert, "Robust Monte Carlo localization for mobile robots", *Artificial Intelligence*, 128 , 99-141, 2001.
- [3] F Lu and E Milios, "Robot pose estimation in planar environments by matching range scans", *Journal of Intelligent and Robotic Systems*, 1997.
- [4] J J Leonard and H F Durrant-Whyte, "Directed Sonar Sensing for Mobile Robot Navigation", *PhD thesis*, University of Oxford, 1992
- [5] Konolige, K. and K. Chou, "Markov Localization by Correlation", *Proc of IJCAI*, 1999
- [6] R. Simmons and S. Koenig. "Probabilistic robot navigation in partially observable environments", *In Proc. of the International Joint Conference on Artificial Intelligence (IJCAI)*, 1995.
- [7] L. Guibas, R. Motwani, and P. Raghavan, *The robot localization problem*, SIAM J. Computing 26 (1997), no. 4, 1120.1138.
- [8] M Rao, G Dudek, and S. Whitesides, "Minimum Distance Localization for a Robot with Limited Visibility", *Proc of ICRA*, 2005
- [9] D Fox, "Adapting the Sample Size in Particle Filters Through KLD-Sampling", *Intl. Journal of Robotics Research*, 22(2), 2003
- [10] H Kose and H L Akin, "The Reverse Monte Carlo Localization Algorithm", *Robotics and Autonomous Systems*, 55, 480-489, 2007.
- [11] C. Kwok, D. Fox, and M. Meila, "Real Time Particle Filters", *Proc of IEEE*, 92(2), 2004
- [12] W. Burgard, D. Fox, and D. Hennig, "Fast grid-based position tracking for mobile robots", *In Proc. of the 21th German Conference on Artificial Intelligence, Germany*. Springer Verlag, 1997
- [13] A K Pandey, K Madhava Krishna and Mainak Nath, "Integrating features onto an occupancy grid for sonar based safe mapping", *IJCAI (International Joint Conference on AI) 2007*



**Fig6a (top):** The map of our research center and the path taken by the robot. Locations where it performed global localization is shown by the points in blue. **Fig6b-6d (middle rows):** Images taken at locations 1,2 and 3, which correspond to the locations denoted in figure 6a. The robot tries to localize at these points. **Fig6e-6g (lower row):** results obtained due to localization at locations 1,2 and 3. It can be seen that the region of highest intensity in figures 6e, 6f and 6g correspond to the locations 1,2 and 3 in figure 6a.